



Experimental and analytical investigation of concrete properties made with recycled coarse aggregate and bottom ash

Ashray Saxena¹ · S. S. Sulaiman² · M. Shariq³ · M. A. Ansari³

Received: 15 April 2023 / Accepted: 6 June 2023 / Published online: 22 June 2023
© Springer Nature Switzerland AG 2023

Abstract

The present study investigates the rebound hammer number (RHN), ultrasonic pulse velocity (UPV), compressive strength, split tensile strength, and modulus of elasticity of concrete made with recycled coarse aggregate and bottom ash. The natural coarse aggregates (crushed rock aggregates) and fine aggregates (sand) are partially or fully replaced (0%, 50%, and 100%) with recycled coarse aggregates (RCA) and coal bottom ash (BA), respectively. Standard concrete specimens were then cast to determine the former properties at 28- and 90-days of curing. The experimentally obtained RCA and BA concrete properties are found comparable to conventional concrete. It has been observed that 100% RCA concrete properties at 90 days are similar to the 28 days of conventional concrete properties. Scanning electron microscope (SEM) analysis has also been performed to examine the mechanism behind the observed properties of RCA, BA, and RCA + BA (concrete containing both RCA and BA) concrete. Based on the experimentally obtained 28-day compressive strength, UPV, and RHN values, the analytical models for predicting the compressive strength, splitting tensile strength, and static modulus of elasticity of RCA, BA, and RCA + BA concrete at any age are also proposed. The values calculated from the proposed models are in good agreement with the experiments. The present study will be helpful for the designers and engineers in practice for fixing preliminary dimensions of concrete elements made with RCA, BA, and RCA + BA concrete mixes, thus leading to sustainable concrete construction.

Keywords Concrete · Recycled coarse aggregate · Bottom ash · Mechanical properties · SEM · Analytical models

Abbreviations

RCA	Recycled coarse aggregate
BA	Coal bottom ash
RCA + BA	Concrete containing both RCA and BA
RHN	Rebound hammer number
UPV	Ultrasonic pulse velocity
SEM	Scanning electron microscope
C&D	Construction and demolition waste
PFA	Pulverized fuel ash
GGBFS	Ground granulated blast furnace slag

ITZ	Interfacial transition zone
OPC	Ordinary Portland cement
w/c	Water-to-cement ratio
C-S-H	Calcium-silicate-hydrate

Introduction

The rapid growth of infrastructural development demands a considerable volume of materials, including steel, concrete, timber, etc. Out of which concrete is one of the most extensively used construction materials for civil engineering projects, such as concrete bridges, dams, multistoried buildings, and rigid pavements, worldwide [1, 2]. A massive quantity of natural resources (stones and sand) is required in such concrete construction. For concrete production, 70–75% volume of aggregates is required in the overall mix, where 60–67% of total aggregates (by volume) constitute coarse aggregate, and the remaining 33–40% constitute fine aggregate. However, the scarcity of virgin aggregates and increasing construction costs using natural resources have posed a

✉ Ashray Saxena
saxena_ashray@utexas.edu

¹ Department of Civil, Architectural and Environmental Engineering, University of Texas at Austin, Austin, TX, USA

² TUM School of Engineering and Design, Technical University of Munich, Munich, Germany

³ Department of Civil Engineering, Z.H. College of Engineering and Technology, Aligarh Muslim University, Aligarh, India

new challenge to design engineers. In the past few decades, several measures to improve the economic and ecological efficiency in the construction sector have been considered to counteract these problems [3]. One is re-using construction and demolition (C&D) waste materials in concrete production, leading to sustainable construction. In recent decades, the quantity of C&D waste has risen due to the expiration of a structure's life, renovation of old structures, or due to wars. These waste materials are disposed of in landfills leading to significant environmental issues. Re-using such material as recycled coarse aggregate (RCA) might be a solution to reduce the burden of C&D waste on landfills while conserving natural resources for concrete production [4]. Though concrete made with recycled coarse aggregate possesses several economic and environmental benefits [5], the greater porosity and higher water absorption capacity of recycled coarse aggregate lower the performance of recycled aggregate-based concrete [6]. Tangchirapat et al. [7] reported that concrete prepared with RCA possesses lower compressive strength, tensile strength, and modulus of elasticity than conventional concrete. Instead, Sagoe-Crentsil et al. [8] showed that concrete prepared with RCA has 12% less abrasion resistance than concrete prepared with natural aggregates. Such behaviors of concrete containing RCA are attributed to RCA's high porosity and water absorption capacity.

In contrast, researchers also used pulverized fuel ash (PFA), ground granulated blast furnace slag (GGBFS), brick, plastic, glass, ceramics, crumb rubber and steel waste materials to improve the strength characteristics of different types of concrete [9–14]. Ann et al. [9] reported that using 30% PFA and 65% GGBFS in concrete containing RCA result in the compressive strength of modified concrete equivalent to the strength of conventional concrete prepared with natural aggregates, while Wang et al. [10] used pozzolanic powders and superplasticizers to improve the mechanical properties of concrete containing RCA. Use of such admixtures resulted in a denser interfacial transition zone (ITZ) in RCA, thereby improving the mechanical behavior of concrete containing RCA. In addition, Ebadi-Jamkhaneh et al. [11] observed the mechanical properties of burnt clay bricks prepared with plastic and steel waste. They concluded that bricks designed with cast iron powder have a higher strength than conventional brick. Another study by Abdellatif et al. [12] concluded that clay brick wastes were helpful for producing sustainable cement bricks. Tahwia et al. [13] used waste materials such as glass, ceramics, and crumb rubber to produce ultra-high-performance geopolymer concrete and found acceptable properties of concrete for different applications. Recently, a detailed survey was carried out by Mohammed et al. [14] and Ahmed et al. [15] on the prediction of mechanical properties, respectively, of geopolymer concrete and concrete composites containing

recycled fibers. They reported that the proposed equations were accurate and could be used to predict geopolymer concrete's mechanical properties. It was also concluded that the different types of recycled fibers could be used in concrete composites to achieve the desired mechanical properties. Moreover, Unis et al. [16] examined that the strength of geopolymer concrete could be increased by adding nano-silica. Singh and Ram [17] revealed that properties of fresh and hardened concrete were improved with the increase in the percentage of fly ash, copper slag, and coal bottom ash in the concrete mixtures. In 2023, Li et al. [18] studied the durability of artificial lightweight coarse aggregate concrete prepared with municipal solid waste incineration bottom ash and three cementitious materials, viz. Portland cement, GGBFS, and fly ash. The authors reported improvement in the durability of modified concrete with reduced CO₂ emissions. Sor et al. [19] also carried out the experimental and analytical study on the strength of lightweight self-compacting concrete prepared with high industrial waste materials. It was found that the strength of lightweight self-compacting concrete decreased with increased polystyrene beads, but the strength value was within the limit specified by American Concrete Institute (ACI).

Developing countries such as India produce large amounts of concrete and manufacture vast quantities of cement, a construction material that contributes to the global carbon footprint. Over the world, the cement industry accounts for 7% of total CO₂ emissions [20, 21]. For this reason, the use of cement is retarded by taking advantage of the pozzolanic properties of different materials like silica fume, fly ash, bottom ash, and rice husk ash. These materials make concrete more environmentally friendly, energy-efficient, and cost-effective. Today, in most countries, fly ash and bottom ash have become popular materials for concrete and embankment construction. Bottom ash is a waste material generated from the coal-based thermal power plant and has much lower pozzolanic properties compared to fly ash, making it unsuitable for cement industries. The bottom ash can be defined as a heterogeneous particle consisting of minerals, magnetic and paramagnetic metals, glass, synthetic and natural ceramics, and unburned materials [22]. Currently, bottom ash gets disposed into the pond, which poses risks to human health and the environment. Additionally, the hazardous constituents of the bottom ash migrate into the groundwater and pose a threat to living organisms [23]. In 2020–2021, India alone produced 232.56 million tons of coal ash on 686.34 million tons of coal in thermal power plants [24]. Hence, it is necessary to safely dispose of bottom ash by substituting it as natural fine aggregate (sand) in concrete construction. Ghafoori and Buchole [25] reported that durable concrete could be prepared by replacing natural fine aggregate with bottom ash. While a study carried out by Aggarwal et al.

[26] suggested that bottom ash concrete mixtures have lower compressive strength than the conventional mix at all curing ages, but the variation in compressive strength after 28 days of curing becomes less distinct. On the other hand, Kim and Lee [27] reported no significant decrease in the strength of bottom ash concrete mixtures compared to concrete containing natural aggregates. However, the modified concrete showed a considerable reduction in the modulus of elasticity after bottom ash incorporation. Recently, Yang et al. [28] concluded that concrete containing bottom ash had less than 3% variation in mechanical properties than conventional concrete.

In the recent decade, studies have been carried out to investigate the combined effect of recycled coarse aggregate and bottom ash on the mechanical properties of concrete [29–31]. Singh et al. [29] used recycled coarse aggregate and bottom ash as substitutes for natural stone and natural sand in self-compacting concrete. They reported 18% and 50% reductions, respectively, in compressive and tensile strengths of concrete prepared with 100% RCA and BA, compared to conventional concrete. Kumar and Singh [30] also investigated the mechanical behavior of self-compacting concrete containing recycled coarse aggregate (0–100%) as a substitute for natural coarse aggregate and 10% bottom ash as a substitute for natural sand. The experimental findings have shown the highest reduction (11%) in the compressive strength of modified concrete at 28 days of curing after incorporating 75% RCA and BA as replacements for conventional aggregates. In addition, the tensile strength of concrete was observed to reduce by 26% compared to conventional concrete after adding RCA and BA. On the other hand, Juric et al. [31] reported that compressive strength of 40 MPa could be achieved even after using RCA and BA as replacements for coarse and fine aggregates, respectively.

Additionally, some researchers also performed multivariable regression analysis by using statistical tools to predict the mechanical properties of concrete containing industrial wastes [32–36]. The proposed empirical relations achieved acceptable agreement between experimental and predicted values.

Based on the previous studies, it has been observed that the RCA and BA have the potential for use in concrete as a partial or total replacement for coarse and fine aggregates, respectively. Most studies have focused on using RCA and BA as natural coarse and fine aggregates at low levels in different types of concrete. Thus, the following key points are the research significance for the present study:

- Limited information is available on using a combination of RCA and BA as a partial or total replacement of coarse and fine aggregate in concrete, respectively, which need

more attention for natural resource conservation and sustainable concrete construction.

- The research hypothesis is to utilize RCA and BA at high volume as coarse and fine aggregate, respectively, in concrete and to examine their effects on concrete's mechanical properties.
- The present experimental study is focused on controlling the use of natural resources such as crushed rock aggregate in concrete construction and resolving the disposal and environmental issues associated with concrete demolition and industrial byproduct wastes.
- Scanning electron microscopy (SEM) analysis has been performed to examine the mechanism behind the mechanical properties of RCA, BA, and RCA + BA concrete, which have not been discussed earlier.
- Analytical solutions based on 28-day compressive strength, UPV, and RHN values have been proposed to predict the compressive strength, splitting tensile strength, and modulus of elasticity of RCA, BA, and RCA + BA concrete at any age.
- The proposed models can predict the strengths and modulus of elasticity of existing concrete structures prepared with RCA, BA, or RCA + BA at any age without knowing the laboratory test results.
- The present study will be helpful for the designers and practicing engineers for fixing preliminary dimensions of concrete elements made with RCA, BA, or RCA + BA concrete mixes.

Experimental design

Materials

The present experimental study chose grade 43 of ordinary Portland cement (OPC) as a binder. The OPC properties conformed to the recommendations of IS 4031 [37] are listed in Table 1. The river sand (locally available) lying in zone-III with fineness modulus and specific gravity of 2.4 and 2.6, respectively, was used as natural fine aggregate, while crushed quartzite rock aggregate of maximum size 20 mm was used as natural coarse aggregate having specific gravity,

Table 1 Physical properties of OPC

Property	Observed value
Specific gravity	3.15
Initial setting time (min)	50
Normal consistency (%)	30
Soundness (%)	2.1
28-day compressive strength (MPa)	43.1



Fig. 1 Coal bottom ash

fineness modulus, and water absorption of 2.67, 6.89, and 1%, respectively. The physical properties of fine and coarse aggregate are satisfied as per IS 383 [38]. The crushing and impact values of natural coarse aggregate were 19% and 17%, respectively.

This study used coal industry-based bottom ash (BA) as a partial or total replacement of riverbed fine aggregate (by weight). The bottom ash was acquired from National Thermal Power Plant (NTPC), Dadri, Uttar Pradesh, India. Figure 1 shows the bottom ash collected from the thermal power plant. On the other hand, the recycled coarse aggregate (RCA) used as a partial or total replacement of natural crushed rock aggregate was acquired from a locally demolished building. Firstly, the concrete blocks were procured (Fig. 2a) from a concrete building demolished after 27 years of age and then transported to the laboratory in plastic bags (Fig. 2b). Finally, the collected material was crushed in the laboratory at ambient temperature to reduce its size as per the size requirement of coarse aggregates in concrete.



Fig. 2 Generation of recycled coarse aggregate: **a** demolished concrete blocks; **b** transportation of concrete blocks in plastic bags; and **c** RCA prepared in the laboratory

Table 2 Particle size distribution of fine aggregate and BA

IS sieves	Fine aggregate				BA			
	Weight retained (gms)	Cumulative weight retained (gms)	Cumulative percent weight retained	Percent weight passing	Weight retained (gms)	Cumulative weight retained (gms)	Cumulative percent weight retained	Percent weight passing
10 mm	0	0	0	100.0	0	0	0	100.0
4.75 mm	180.0	180.0	6.0	94.0	0.0	0.0	0.0	100.0
2.36 mm	240.0	420.0	14.0	86.0	150.0	150.0	5.0	95.0
1.18 mm	270.0	690.0	23.0	77.0	210.0	360.0	12.0	88.0
600 micron	450.0	1140.0	38.0	62.0	580.0	940.0	31.3	68.7
300 micron	830.0	1970.0	65.7	34.3	1640.0	2580.0	86.0	14.0
150 micron	840.0	2810.0	93.7	6.3	360.0	2940.0	98.0	2.0
Pan	190.0	3000.0	100.0	0.0	60.0	3000.0	100.0	0.0

Table 3 Particle size distribution of natural coarse aggregate and RCA

IS sieves	Coarse aggregate				RCA			
	Weight retained (gms)	Cumulative weight retained (gms)	Cumulative percent weight retained	Percent weight passing	Weight retained (gms)	Cumulative weight retained (gms)	Cumulative percent weight retained	Percent weight passing
80 mm	0	0.0	0.0	100.0	0	0	0	100
40 mm	0	0.0	0.0	100.0	0	0	0	100
20 mm	210.0	210.0	4.2	95.8	250.0	250.0	5.0	95.0
10 mm	4030.0	4240.0	84.8	15.2	3555.0	3805.0	76.1	23.9
4.75 mm	760.0	5000.0	100.0	0.0	1195.0	5000.0	100.0	0
Pan	0	5000.0	100.0	0.0	0.0	5000.0	100.0	0

Table 4 Physical properties of coal bottom ash and recycled coarse aggregate

Property	Observed value	
	BA	RCA
Specific gravity	2.28	2.65
Fineness modulus	2.32	6.81
Water absorption (%)	14.8	1.8
Color	Black grey	–
Crushing value (%)	–	18
Impact value (%)	–	16

Figure 2c shows the crushed aggregates used as recycled coarse aggregates to prepare modified concrete. The particle size distribution of fine aggregate and BA, natural coarse aggregate and RCA is given in Tables 2 and 3, respectively, as per IS 383 [38]. The physical properties of BA and RCA are listed in Table 4.

Mix design

A total of seven concrete mixes were prepared in the present study. Firstly, the conventional (i.e., control) concrete mix containing natural coarse and fine aggregate of M25 grade was designed using the trial method, considering the guidelines of IS 10262 [39], and designated as M1. The mix M1 was then re-proportioned by replacing only natural coarse aggregate with 50% and 100% RCA to obtain RCA concrete mixes, designated as M2 and M3, respectively. In addition, re-proportioning of the M1 mix was done again by replacing only fine aggregate with 50% and 100% BA to obtain BA concrete mixes, designated as M4 and M5, respectively. Finally, mix M1 was modified by replacing both coarse and fine aggregates with 50% and 100% RCA and BA, respectively, and the mixes were designated M6 and M7. M6 and M7 concrete mixes are developed to investigate the combined effect of the high percentage of RCA and BA on the performance of conventional concrete. Moreover, the

quantity of cement and water-to-cement (w/c) ratio were not changed for all concrete mixes to examine only the effect of fine and coarse aggregate replacement, respectively, with BA and RCA on the mechanical properties of concrete containing different percentages of BA and RCA. Initially, coarse aggregates (i.e., 0%, 50%, and 100% RCA) in saturated surface dry condition and fine aggregates (i.e., 0%, 50%, and 100% BA) were mixed thoroughly, and then, the required amount of cement was added. A mixer was used to prepare the uniform dry mix, where mixing was carried out for at least one minute. The required dosage of water was then added gradually to the prepared dry mix, and the mixer was rotated for two minutes to produce a cohesive mix. It should be noted that standard molds of 100 mm × 200 mm (internal diameter × internal height) dimensions were filled with concrete mixes in three layers, where each layer was compacted using vibratory table to maintain the consistency and density of compacted concrete. The mix proportions of the concrete mixtures evaluated in this study are listed in Table 5.

Specimen preparation and testing

In this study, cylindrical concrete specimens of dimensions 100 mm × 200 mm (diameter × height) were prepared to evaluate the concrete mixes' 28-day and 90-day mechanical properties. All the concrete specimens were taken out of the cylindrical mold after 24 h of casting followed by curing underwater or under submerged curing conditions for 28 and 90 days, as shown in Fig. 3a. A standard laboratory temperature, i.e. (27 ± 2 °C), was maintained during the preparation and curing of concrete specimens. After 28 and 90 days of curing, non-destructive testing was performed on all the concrete specimens evaluated in this study. The ultrasonic pulse velocity was measured using the UPV tester, as shown in Fig. 3b. The UPV tester was made by Proceq, Switzerland, with the accessories including 58E-48 ultrasonic tester, 54 kHz type, two transducers (one receiver and one transmitter head), connecting cables, a rod for calibration, a coupling agent for filling any pores on the surface

Table 5 Concrete mix proportions

Mix ID	Replacement of RCA (%)	Replacement of BA (%)	RCA (kg/m ³)	BA (kg/m ³)	Cement (kg/m ³)	w/c ratio	Fine aggregate (kg/m ³)	Coarse aggregate (kg/m ³)
M1	0	0	0	0	422	0.45	576	1168
M2	50	0	584	0			576	584
M3	100	0	1168	0			576	0
M4	0	50	0	288			288	1168
M5	0	100	0	576			0	1168
M6	50	50	584	288			288	584
M7	100	100	1168	576			0	0

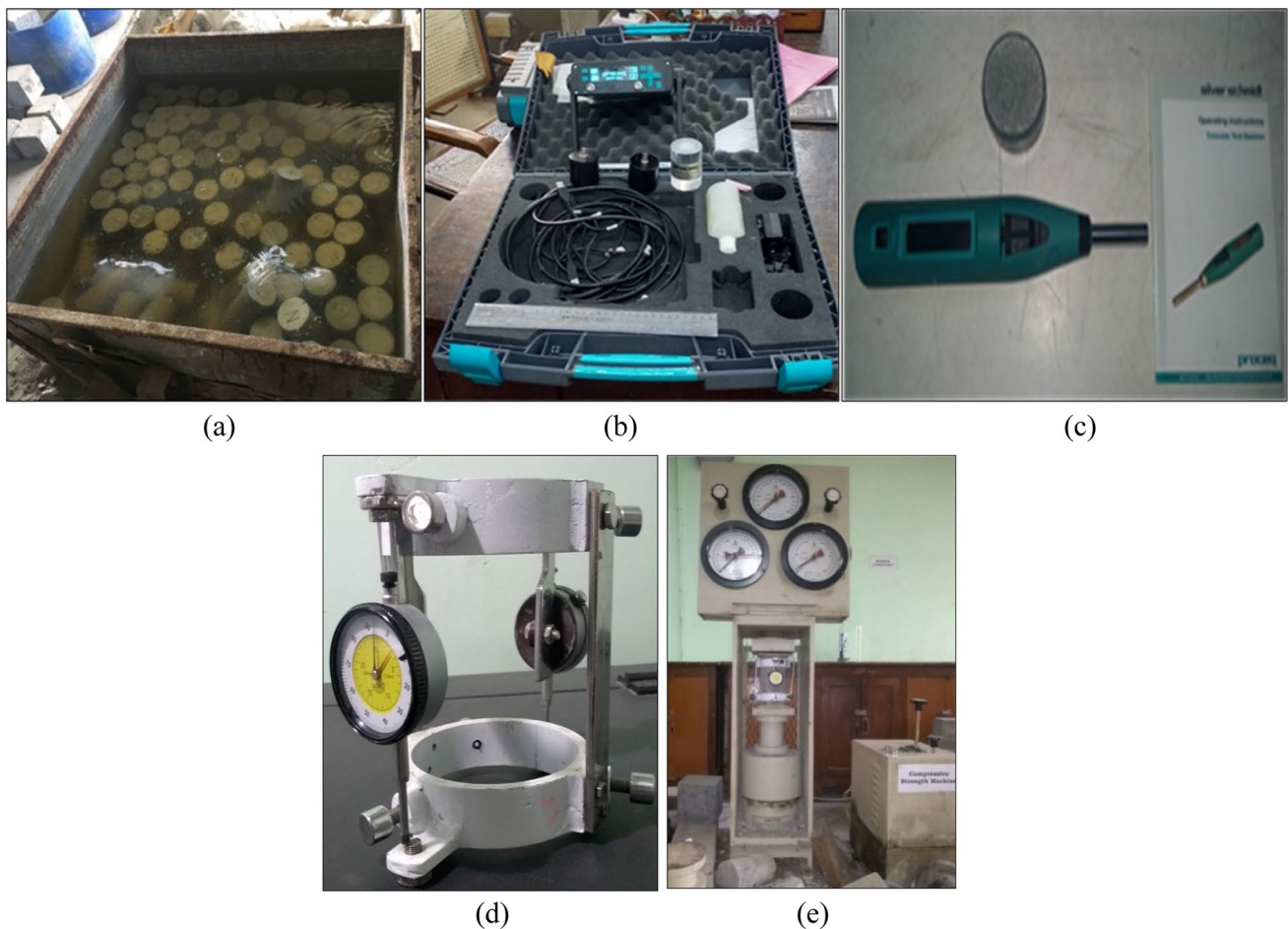


Fig. 3 Details of preparation and testing of concrete specimens: **a** curing of specimens; **b** UPV tester with accessories; **c** Schmidt's rebound hammer; **d** compressometer; and **e** compression testing machine

of specimens to provide proper contact between transducers and surfaces of the specimen and two 1.5-V alkaline D-type batteries. On the other hand, the rebound hammer number (RHN) was measured with the help of a rebound hammer device made by Proceq, Switzerland, as shown in Fig. 3c. The RHN tester had the specifications as 2.207 Nm

(N) and 0.735 Nm (L) impact energy, 115-g hammer mass, 0.79 N/mm (N), and 0.26 N/mm (L) spring constant, 75 mm spring extension, and dimensions of the hammer were 55 × 55 × 250 mm (340 mm to the tip of the plunger). The plunger dimensions were 105 × 15φ mm/radius of a spherical tip, 25 mm, and 600 g weight. Once the non-destructive

testing on the concrete specimens was completed, the specimens were tested in destructive testing, i.e., under compression for determination of compressive and splitting tensile strength as per the guidelines of IS 516 [40] and IS 5816 [41], respectively. The test for determining the elastic modulus of concretes evaluated in this study was performed according to ASTM C469 [42]. A compressometer with two dial gauges (with the least count of 0.01 mm), shown in Fig. 3d, was used to measure the longitudinal strain in concrete specimens subjected to compression in a compression testing machine. The capacity of the compression testing machine, as shown in Fig. 3e, was 200 tons and was used to determine the mechanical properties of conventional and modified concrete mixtures. While determining the compressive and indirect tensile strength of concrete mixtures, the load on the specimens was increased gradually at a loading rate of 14 N/mm² per minute. During testing, the load and displacements are recorded to obtain the maximum load resisted by each mixture to calculate the respective compressive and indirect tensile strength of given concrete specimen. Finally, the elastic modulus of concrete specimens was measured using the secant modulus, which was obtained by joining two points on the stress–strain curve, i.e., by joining the origin to the point of 40% of ultimate compressive strength (f'_c) of respective concrete ($0.4f'_c$). The results of the mechanical properties of each mixture and at different ages were summarized based on the average of five specimen readings. In addition, a microscopic study was performed using a scanning electron microscope (SEM) to understand the microstructure of concrete containing recycled coarse aggregate and bottom ash. SEM images were used to analyze the presence of micro-cracks and pores within the concrete structure for all the tested concrete specimens. The SEM analysis was conducted on crushed pieces of specimens obtained after the destructive testing. The obtained crushed pieces were first coated with gold prior to observation.

Results and discussions

Quality check of concrete made with RCA and BA using non-destructive testing

The results of the Schmidt rebound hammer test for concretes containing different percentages (0, 50, and 100%) of recycled coarse aggregate and bottom ash are presented in Fig. 4a. As per the guidelines provided by IS 13311-Part II [43], it should be noted that a rebound number less than 20 denotes poor quality concrete, while a value more than 40 indicates a very good hard layer of concrete. For the concrete mixtures prepared in this study, the Rebound number was observed in the range of 23–30, thereby indicating the quality of concrete to be fair and good. The rebound number of

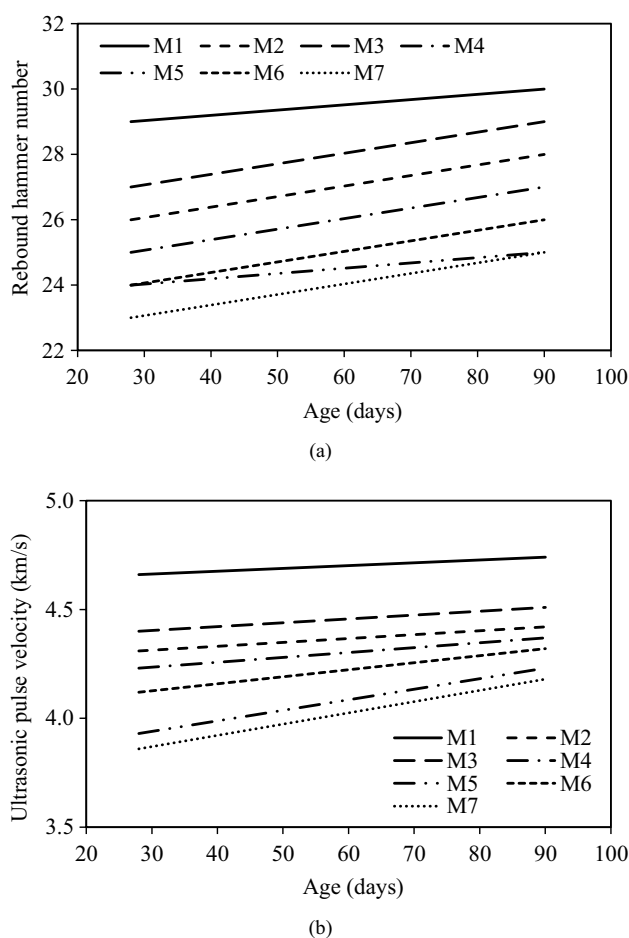


Fig. 4 Rebound hammer number and ultrasonic pulse velocity results of concretes evaluated in this study: **a** rebound hammer number versus curing age; and **b** ultrasonic pulse velocity versus curing age

control specimen at all curing ages is the highest compared to other concrete mixtures evaluated in this study because of the uniform mixing of constituents of the control mix. However, with the increase in the curing age, i.e., at 90 days of curing, the rebound number of concrete containing 100% RCA achieved the good hard layer concrete range. The reason behind getting the higher rebound number for concrete prepared with 100% RCA than concrete having 50% RCA may be attributed to the hydration of old mortar paste available on the surface of RCA.

In contrast, the replacement of natural sand with bottom ash influenced the bond between the constituents of concrete. Thus, it resulted in a lower rebound number compared to that of M1, M2, and M3 concrete mixes. Investigations have shown that bottom ash particles are more porous and weaker than natural sand particles [44], which results in higher water demand for the mixes. The demand for higher w/c results in a low density of aggregate, and the trapped water in the mix results in the formation of small pores near the aggregate surface. These pores prevent the bonding

between the cement paste and aggregates, resulting in a lower rebound number. In the present study, the rebound number of concrete containing 100% RCA and BA is lowest than other mixes. The reason is the interference of bottom ash particles with RCA particles, which might have resulted in poor interfacial bonding between the cement mortar and aggregate, ultimately affecting the hydration of old mortar, thus reducing the rebound number.

BS1881 [45] suggested that the rebound number indicates the hardness of concrete only up to 30 mm depth from the tested surface. As per IS 13311-Part II [43], if the concrete has internal micro-cracks, flaws, or heterogeneity across the cross-section, the rebound hammer number will not indicate the same. Teodoru [46] further suggested that the rebound number indicates the strength of the outer concrete layer up to a depth of 30–50 mm. In one of the previous studies, Neville [47] concluded that the rebound hammer test should not be used alone to determine the strength of concrete. Hence, the UPV test is performed to examine the reliability of the concrete mixtures.

Figure 4b presents the UPV test results at 28 and 90 days of curing for concretes evaluated in this study. The UPV figures for all combinations were varied from 3.86 km/s to 4.74 km/s. By comparing the obtained results with the range of UPV given in IS 13311-Part I [48], it is pointed out that all the concrete mixtures are in the range of good to excellent quality concrete. However, in the concrete containing both RCA and BA, increasing the substitution level to 100% caused a reduction of 17.2% (at 28 days) and 11.8% (at 90 days) in UPV values compared to that of the control concrete. The UPV value of concrete mixtures containing RCA and BA has been reduced due to the higher porosity of RCA and BA aggregates than natural crushed limestone and sand aggregates. Khatib [49] also reported 8.8% reduction in UPV values for the mixtures containing 100% fine recycled concrete aggregate. As expected, the UPV value of concrete containing 100% RCA is higher than that of the concrete containing 50% RCA due to the hydration of old mortar in the RCA specimens, based on a study carried out at the microscopic scale by Gholampour et al. [50]. Finally, the UPV test results are found in a similar pattern as discussed for the rebound hammer test, suggesting the same hypothesis for all concrete mixes.

Mechanical properties of concrete made with RCA and BA

Figure 5a highlights the compressive strength of the concrete mixes evaluated in this study with increased curing age. The conventional concrete yielded the highest compressive strength at 28- and 90-days, 27 MPa and 29 MPa, respectively. Meanwhile, the compressive strength of concrete containing RCA, BA, and their combination is lower

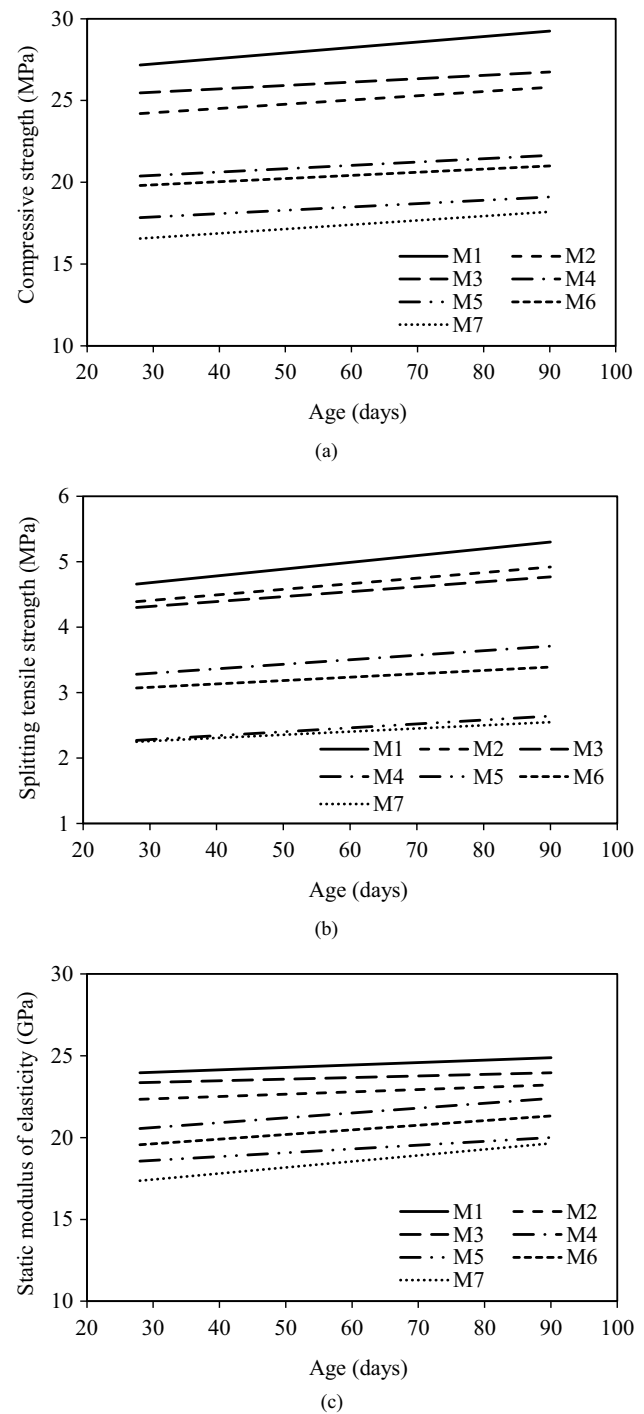


Fig. 5 Results of compressive strength, tensile strength, and modulus of elasticity of concretes evaluated in this study: **a** compressive strength versus curing age; **b** splitting tensile strength versus curing age; and **c** static modulus of elasticity versus curing age

than conventional concrete at all curing ages. This could be attributed to the fact that the presence of old-adhered mortar on RCA and BA in mixes caused poor bonding between the cement paste and aggregates and ultimately increased the

water absorption capacity of the mixes leading to less dense mix with pores near the aggregate surface [7, 8]. In addition, concrete containing 100% RCA and BA exhibited the lowest compressive strength amongst all the concrete mixtures being tested at 28 and 90 days of curing. A similar trend has been reported by Kumar and Singh [30], where the compressive strength of concrete decreased after replacing coarse and fine aggregates with RCA and bottom ash, respectively. However, a sudden jump in compressive strength of concrete containing 100% RCA and BA was observed from 28 to 90 days of curing age. The compressive strength of concrete containing 100% RCA and BA was found to increase by 9.9% when the curing age of concrete was increased from 28 to 90 days. On the other hand, the increase in the compressive strength of conventional concrete from 28 to 90 days of curing was only 7.7%. The delay in hydration and slow pozzolanic activity of concrete containing RCA and BA may explain their significant increase in compressive strength with an increase in curing age. This trend is similar to the research conducted by Cheriaf et al. [51] and Singh and Bharadwaj [52], where the compressive strength of concrete incorporating bottom ash increased with increased curing time due to the pozzolanic reaction process at a later stage.

Moreover, concrete should resist tensile forces during its design life. The tensile strength of the concrete mixtures was examined indirectly by determining the splitting tensile strength of the mixes. The results of tensile strength at 28 and 90 days of the concrete mixtures evaluated in this study are shown in Fig. 5b. Concrete containing RCA and BA displays a similar trend in developing tensile strength as compressive strength. The general trend suggests that the tensile strength of conventional, RCA, and BA concrete declines as the replacement level of natural aggregate by the RCA and BA increases. Concrete mixtures blended with 100% RCA and BA demonstrated the lowest tensile strength at all ages compared to other mixes. The 28-day splitting tensile strength of M6 and M7 concrete mixtures is 65.9% and 48.3%, respectively, of conventional concrete. In comparison, the 90-day splitting tensile strength of the M6 and M7 concrete mixture is 72.7% and 54.7%, respectively, of 28-day conventional concrete strength. Hence, a prolonged curing period allowed better pozzolanic reaction in concrete specimens containing RCA and BA for a higher generation of binding gel that assisted in strength development with an increase in curing age [53].

From the literature published, it is clear that the use of RCA and BA significantly affects the modulus of elasticity of concrete. In general, the modulus of elasticity decreases with the increase in coarse and fine aggregate replacement levels. Figure 5c presents the results of the elastic modulus of concrete mixtures evaluated in this study at 28 and 90 days of curing. As can be seen in the figure, the concrete's elastic modulus increases with curing age, irrespective of

the concrete mixture. The elastic modulus of concrete containing RCA, BA or their combination is lower than the conventional concrete at all curing ages, regardless of the percentage replacement of natural coarse and fine aggregate and curing age. The figure shows that the elastic modulus of mix containing 100% RCA and BA is the lowest among all the concrete mixtures being tested in the laboratory. From 28- to 90-days of curing, the elastic modulus of M2 and M3 concrete mixtures varies from 93–97% to 97–100%, respectively, of the 28-day elastic modulus of control concrete. Similarly, for M4 and M5 concrete mixtures, the elastic modulus varies from 86–93% to 77–83%, respectively, while for M6 and M7 concrete mixtures, this value is 82–89% and 72–82%, respectively. The porous nature and lower stiffness of the old mortar and bottom ash are responsible for the decrease in the modulus of elasticity of concrete containing RCA and BA. In a study conducted by Andrade et al. [54], concrete with 100% BA resulted in 34% reduction in modulus of elasticity than concrete produced with natural sand. Nakararoj et al. [55] also reported decreased elastic modulus after addition of RCA and BA to high-strength concrete.

Strength development with time

In concrete construction, the development of strength with time plays an essential role in achieving the desired or practical value of design strength. The graphical presentation of experimental values of compressive and splitting tensile strength are put forward in Fig. 5a and b, respectively. From the results, it has been observed that the compressive strength development from 28 to 90 days for M1 M2, M3, M4, M5, M6, and M7 concrete mixes is 7.66%, 6.65%, 5.03%, 6.23%, 7.12%, 6.06%, and 9.90%, respectively. Similarly, the splitting tensile strength development from 28 to 90 days for M1 M2, M3, M4, M5, M6, and M7 concrete mixes is 13.10%, 12.07%, 10.93%, 13.11%, 16.30%, 10.42%, and 13.33%, respectively. This shows that the maximum compressive strength development is achieved in the M7 concrete mix prepared with 100% RCA and BA replacement. In contrast, the maximum splitting tensile strength development is observed in the M5 concrete mix with 100% BA replacement. Thus, from compressive strength point of view, the optimum mix is M3 among all RCA and BA concrete mixes (since the strength of M3 and M1 mixes are close to each other). Whereas from compressive strength development viewpoint from 28 to 90 days, the optimum mix is M7 among all concrete mixes evaluated in this study, including the conventional concrete mix.

Microstructure analysis

The inherent microstructure of concrete made with recycled coarse aggregate and bottom ash affects its mechanical

properties. The hydration time, replacement percentage of coarse and fine aggregates, and cement type (hardened or fresh) all significantly affect the microstructure of conventional concrete. In order to perform microstructure analysis, images of broken concrete pieces (obtained after compressive strength determination) mounted on SEM stub were taken. The microstructural analysis using scanning electron microscopy (SEM) supported and justified the experimental results. Figure 6 shows the SEM images of the control mix after 90 days of curing in the magnification of 500x, 2500x, and 7000x used to compare the microstructure analysis of concrete containing either or both recycled coarse aggregate and bottom ash. The SEM image of the control mix shows the calcium–silicate–hydrate (C–S–H) gel within the matrix of concrete and dense structure with fewer microcracks and pores.

Figure 7a and b shows the SEM images at the cut surface of concrete containing recycled coarse aggregate, i.e., after 50% (M2) and 100% (M3) natural coarse aggregate replacement, respectively, at 90 days of curing. The figure shows microcracks and micropores on the old mortar surface attached to RCA, which might have resulted in the inferior quality of the M2 and M3 concrete mixtures. Mistri et al. [56] reported that these cracks develop the initial fracturing zone at the interface of new mortar and RCA, resulting in poor-quality concrete containing RCA. Yap et al. [57]

conducted a microstructure analysis on recycled concrete aggregate and found that the failure of concrete containing recycled coarse aggregate predominantly occurs at the interface between the recycled coarse aggregate particles and the adhered mortar. This is due to the accelerated crack propagation facilitated by the presence of weaker mortar adhered to the RCA. In this study, M3 concrete mixtures rendered higher strength than M2 concrete mixtures. This might be due to the further hydration of old mortar available on the surface of recycled coarse aggregate, resulting in improved bonding between RCA and new cement mortar. In addition, ettringite crystals that appear in the form of needle in M3 concrete mixtures resulted in a stronger bond between the old cement paste and aggregate.

The SEM images of concrete mixtures at 90 days of curing having natural sand replaced with BA, i.e., after 50% (M4) and 100% (M5) replacement of fine aggregate with BA, can be seen in Fig. 7c and d, respectively. It can be seen in SEM images of concrete containing BA that microscopic air gaps were formed due to the absorption of water by bottom ash particles. When natural river sand is substituted with BA, the microstructure changes the network structure of the concrete. Specifically, the structure of the modified concrete becomes more porous than the control concrete. Moreover, utilization of bottom ash leads to detachment of grains in the structure of concrete [58]. The formation of discrete grains

Fig. 6 SEM images of the control mix after 90 days of curing

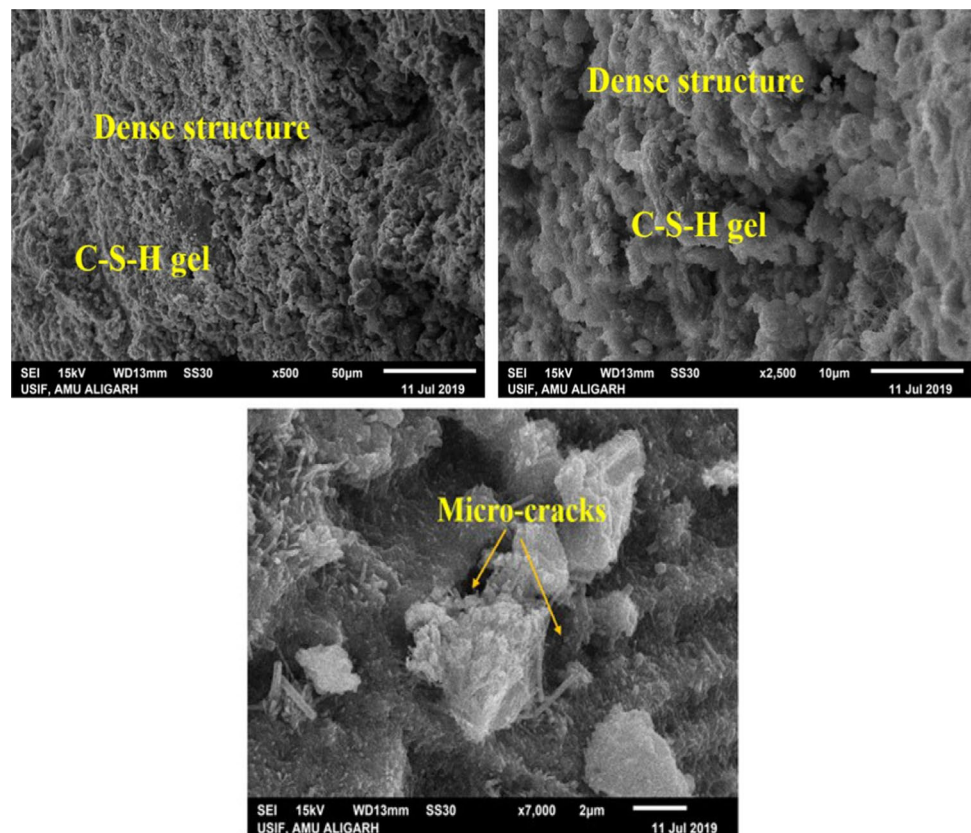
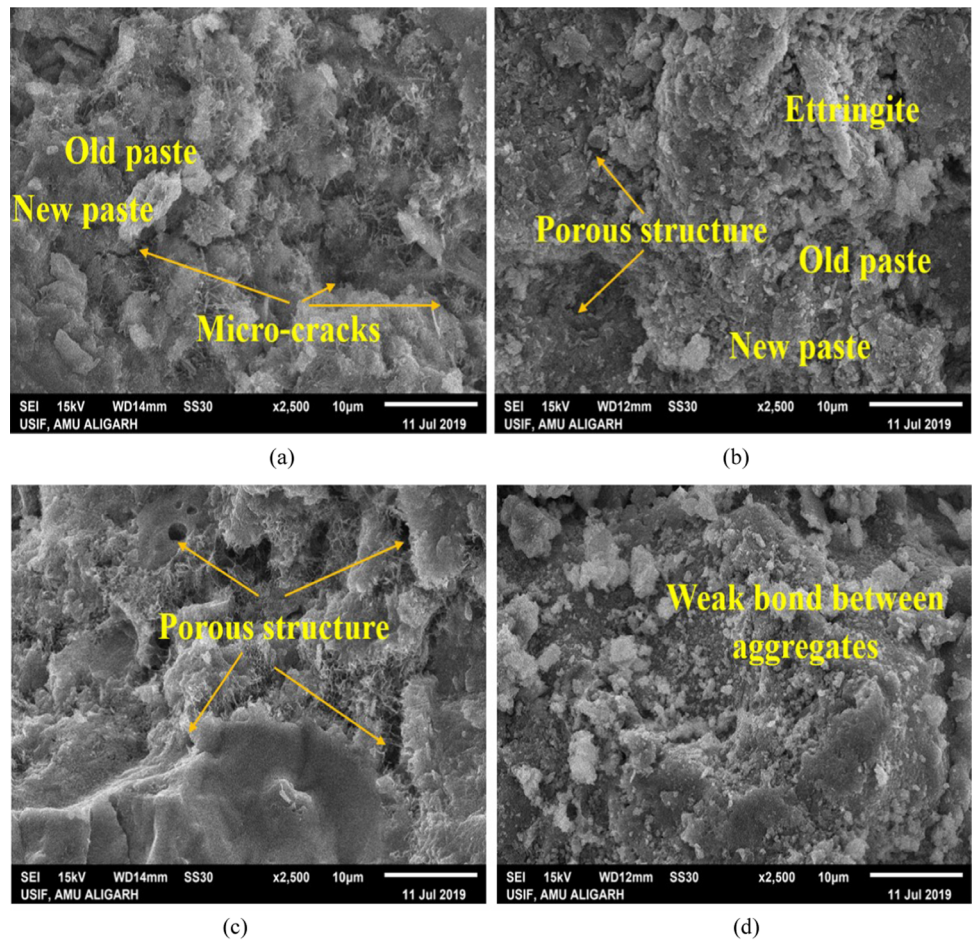


Fig. 7 SEM images of concrete mixtures containing either recycled coarse aggregate or bottom ash: **a** concrete with 50% RCA; **b** concrete with 100% RCA; **c** concrete with 50% BA; and **d** concrete with 100% BA

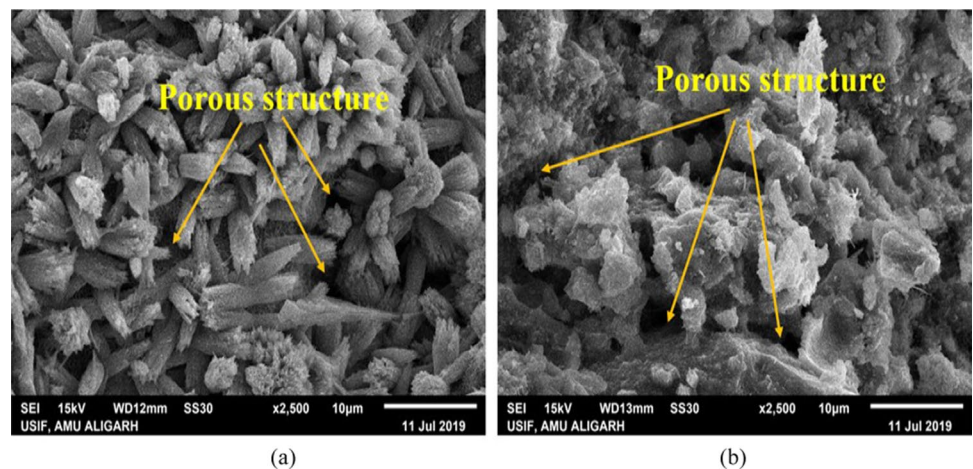


and the porous area close to the aggregate surface might be the leading cause of reduction in the compressive strength, tensile strength, and modulus of elasticity of concrete prepared with BA [58]. Additionally, the microstructure of concrete containing bottom ash is observed different from control mix due to the sluggish pozzolanic activity of coal

bottom ash, which causes a modest reduction in strengths of concrete during early curing stages.

Finally, the microstructure of M6 and M7 concrete mixtures is obtained, as shown in Fig. 8a and b. In Fig. 8a and b, with reference to 50% and 100% replacement of coarse and fine aggregate, a large number of porous spaces and microcracks can be observed in the mortar section, resulting

Fig. 8 SEM images of concrete containing both recycled coarse aggregate and bottom ash: **a** concrete with 50% RCA and BA; **b** concrete with 100% RCA and BA



in poorer interfacial bonding between the aggregate and the cement pastes. Similar observations have been revealed in past studies conducted by Abdellatif et al. [59, 60] and Tahwia et al. [61]. In addition, the presence of large void spaces in concrete mixtures incorporating both RCA and BA results in the development of a weak interfacial transition zone (ITZ) between the old and new mortar. Consequently, the overall strength of such concrete mixtures reduces due to the presence of this additional vulnerable connection [51]. Singh and Siddiqui [62] used bottom ash with foundry sand and suggested that C–S–H gel was not widely spread in the mix after addition of porous bottom ash into the concrete mixture. Thus, BA concrete was observed to have lower strength than conventional concrete. Overall, in this study, the mechanical properties of concrete mixtures may have been influenced by the formation of weak C–S–H gel, resulting from the incorporation of RCA and BA into the concrete mixtures, as well as the porous characteristics of the old mortar and BA. This observation is similar to the work of Rafieizonooz et al. [63], where porosity and weak C–S–H gel reduced the compressive strength of concrete after the replacement of sand by BA.

Analytical solutions

The analytical models for predicting age-dependent mechanical properties (i.e., compressive strength, splitting tensile strength, and elastic modulus) of concrete containing RCA, BA, or RCA + BA are needed to minimize the construction time and monitor the health of the existing structures. The results from the experimental investigations for concretes containing either or both RCA and BA are obtained different than the results of control concrete. The reason may be the poor bonding between the old and new mortar and variation in the properties of recycled coarse aggregate and bottom ash. Therefore, in this study, new analytical models for predicting mechanical properties (i.e., compressive strength, splitting tensile strength, and elastic modulus) of concrete containing either or both recycled coarse aggregate and bottom ash at any time have been proposed based on crushing strength, UPV and RHN values of concrete mixtures. A multivariable regression analysis has been carried out using the hyperbolic expression to develop the models given in Eqs. (1–9) to predict strengths and modulus of elasticity of RCA, BA, and RCA + BA concrete. The hyperbolic expression given in the statistical tool (i.e., sigma plot) was modified by incorporating the input parameters such as the age of concrete, 28-day compressive strength, RHN, UPV, percentage of RCA, BA, and RCA + BA considered in the present study [33, 34]. Faraj et al. [35] also used the statistical tool to predict the compressive strength of self-compacting concrete containing recycled plastic aggregates and industrial waste

ashes, while Ahmed et al. [36] used it for the prediction of strength of geopolymer mortar. The models proposed in the present study are applicable to OPC-based concrete mixes containing different percentages of RCA, BA, and their combination. However, further analysis is required for prediction of strengths of other type of concretes such as geopolymer concrete when containing RCA, BA, or their combination.

Age-dependent models for prediction of compressive and tensile strength of concrete containing either or both RCA and BA

The proposed models to predict the compressive strength of concrete at any age based on the 28-day crushing compressive strength of conventional concrete, UPV, and RHN values are shown in Eqs. (1), (2) and (3). Equation (1) predicts the compressive strength at any age of concrete mixtures containing different percentages of RCA and BA through destructive testing on control concrete mixture, i.e., by performing compressive strength test on conventional concrete mixture in the laboratory after 28 days of curing. On the other hand, the models given in Eqs. (2) and (3) are applicable to the onsite inspection of concrete structures containing different percentages of RCA and BA, where the structural health of the buildings can be measured through non-destructive testing. Since during structural health monitoring, it is not possible to determine the strength of concrete based on a crushing test by taking a core from the existing structure, the proposed models given in Eqs. (2) and (3) will help in determining the strength of concrete structures containing different percentages of RCA and BA by using UPV and RHN values only.

$$(f'_c)_t = \frac{\exp(C_3 p_{\text{rca}} + C_4 p_{\text{ba}}) t (f'_c)_{28, \text{plain}}}{C_1 + C_2 t} \quad (1)$$

$$(f'_c)_{t, \text{UPV}} = \frac{C_{10} \exp(C_7 p_{\text{rca}} + C_8 p_{\text{ba}} + C_9 \text{UPV}) t}{C_5 + C_6 t} \quad (2)$$

$$(f'_c)_{t, \text{RHN}} = \frac{C_{16} \exp(C_{13} p_{\text{rca}} + C_{14} p_{\text{ba}} + C_{15} \text{RHN}) t}{C_{11} + C_{12} t} \quad (3)$$

where $(f'_c)_t$ = concrete compressive strength at age 't' of cylindrical specimen (MPa); t = concrete age in days; $(f'_c)_{28, \text{plain}}$ = 28-day conventional concrete compressive strength in MPa of the cylindrical specimen; p_{rca} = recycled coarse aggregate percentage in fraction; p_{ba} = percentage of bottom ash in fractions; $(f'_c)_{t, \text{UPV}}$ = concrete compressive strength at age 't' using UPV in MPa; $(f'_c)_{t, \text{RHN}}$ = concrete

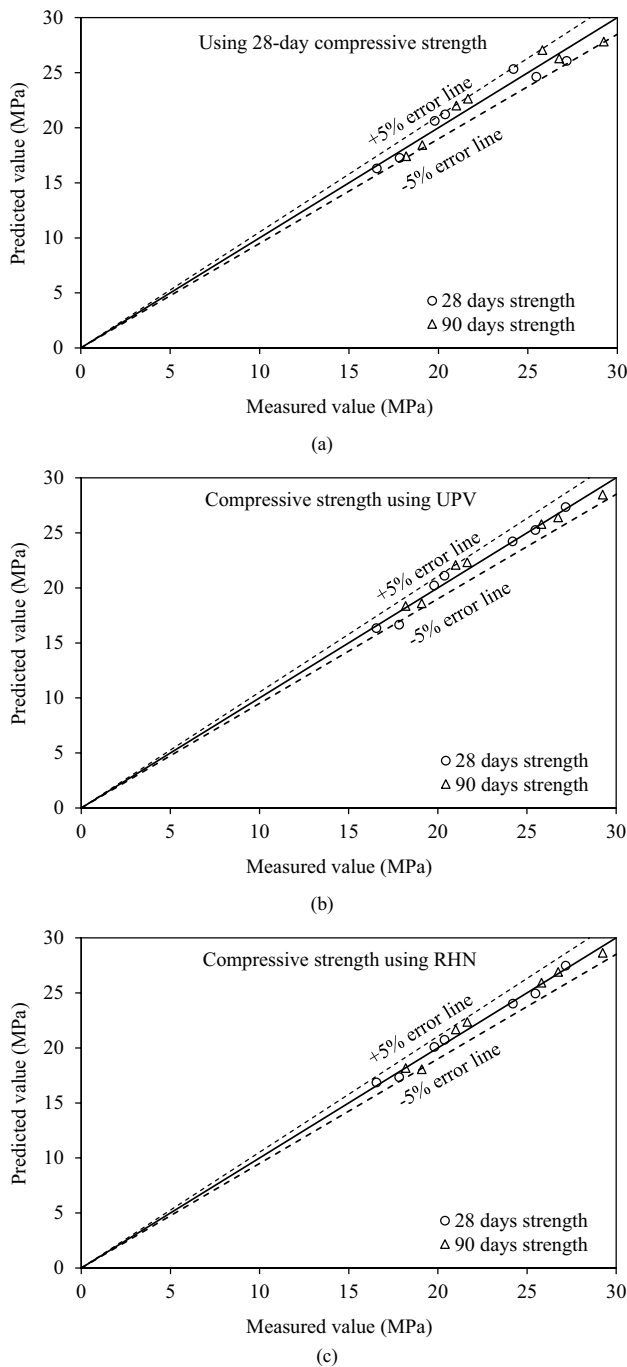


Fig. 9 Comparison between measured and predicted compressive strength of concretes evaluated in this study: **a** prediction using 28-day crushing compressive strength; **b** prediction using UPV; and **c** prediction using RHN

compressive strength at age ‘*t*’ using RHN in MPa; C1 to C16 = model parameters having values 2.675,

0.947, −0.056, −0.412, 0.591, 0.918, 0.003, −0.266, 0.315, 5.921, 0.034, 0.118, 0.006, −0.290, 0.034 and 1.215, respectively.

Figure 9a–c shows a comparison of the experimental and predicted compressive strength of concretes evaluated in this study based on $(f'_c)_{28,plain}$, UPV and RHN values [i.e., using Eqs. (1), (2), and (3)], respectively. The figures show that 100%, 87.5%, and 94.0% of the data points fall within an error band of $\pm 5\%$ for the compressive strength prediction using Eqs. (1), (2), and (3), respectively. The acceptability of these models can also be justified with R^2 values, obtained as 0.94, 0.98, and 0.98 for Eqs. (1), (2), and (3), respectively. From the above model prediction analysis, it can be suggested that the concrete compressive strength can be predicted using Eqs. (2) and (3) based on UPV and RHN values, respectively, for any percent replacement of RCA and BA. In addition, these models can be applied to existing concrete buildings to assess their residual strength without knowing the laboratory’s 28-day compressive strength based on the crushing test.

The analysis of experimental results and the empirical relationships in design codes of different countries revealed that compressive strength could play an essential role in predicting the splitting tensile strength (f_{spt}) of concrete mixtures. However, an age-dependent model for predicting the splitting tensile strength of concrete prepared with RCA and BA is still needed based on compressive strength at 28 days, UPV, and RHN values of the respective concrete mixtures. Thus, based on the multivariable regression analysis and by using models given in Eqs. (1), (2), and (3), the following models presented in Eqs. (4), (5), and (6) have been proposed for predicting the splitting tensile strength of concrete containing different percentages of RCA and BA.

$$(f_{spt})_t = k_1 [(f'_c)_t]^{K_2} \tag{4}$$

$$(f_{spt})_{t,UPV} = k_3 [(f'_c)_{t,UPV}]^{K_4} \tag{5}$$

$$(f_{spt})_{t,RHN} = k_5 [(f'_c)_{t,RHN}]^{K_6} \tag{6}$$

where $(f_{spt})_t$ = concrete splitting tensile strength at age ‘*t*’ in GPa; $(f_{spt})_{t,UPV}$ = concrete splitting tensile strength at age ‘*t*’ using UPV in GPa; $(f_{spt})_{t,RHN}$ = concrete splitting tensile strength at age ‘*t*’ using RHN in GPa; k_1 to k_6 = model parameters having values 0.021, 1.661, 0.026, 1.594, 0.028, and 1.568, respectively.

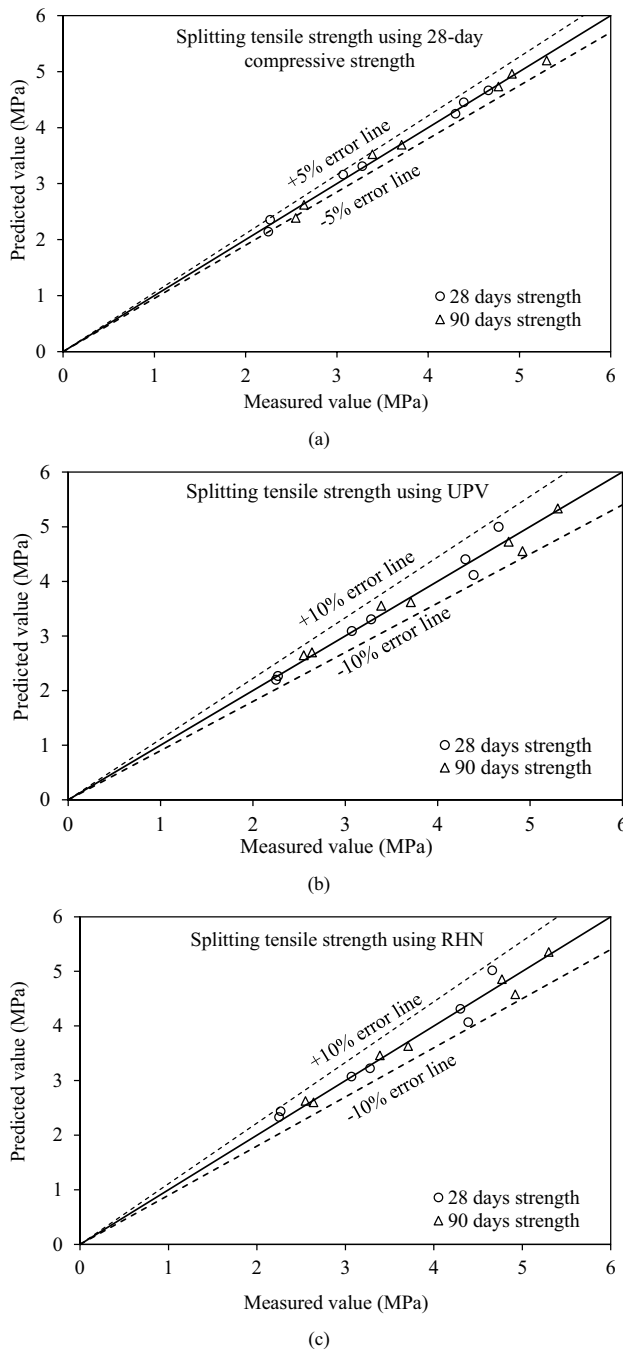


Fig. 10 Comparison between measured and predicted splitting tensile strength of concretes evaluated in this study: **a** prediction using 28-day compressive strength; **b** prediction using UPV; and **c** prediction using RHN

The comparative analysis between the predicted and measured values of splitting tensile strength for concrete mixes evaluated in this study based on 28 days of conventional concrete compressive strength, UPV, and RHN is presented in Fig. 10a–c, respectively. From the figures, it seems that 100% of the data points lie within the error band $\pm 5\%$, $\pm 10\%$, and $\pm 10\%$

in the prediction of splitting tensile strength using the proposed models given in Eqs. (4), (5), and (6), respectively. Thus, it can be said that the proposed models for predicting the splitting tensile strength of concrete containing different percentages of RCA and BA are in acceptable agreement with the measured data.

Age-dependent models for prediction of elastic modulus of concrete containing either or both RCA and BA

The current state of the art on the static elastic modulus (E_c) of concrete indicates the need for a new model to predict the age-dependent elastic modulus of concrete containing different percentages of RCA and BA. Moreover, age-dependent formulae for E_c of concrete proposed by researchers and empirical relationships proposed by design codes of various countries are silent on the effect of RCA and BA on the elastic modulus of conventional concrete, and its prediction based on UPV and RHN values has not yet been explored. Therefore, a multivariable regression analysis has been performed to propose new age-dependent models for predicting the static elastic modulus of concrete for any percentage replacement of natural crushed rock and riverbed aggregate with RCA and BA, respectively. As shown in Eq. (7), a model can predict the static elastic modulus of RCA- and BA-based concrete at any age using 28 days of conventional concrete compressive strength. Similarly, the models depicted in Eqs. (8) and (9) have been proposed for predicting the static elastic modulus of RCA- and BA-based concrete at any age using UPV and RHN values, respectively. Thus, it can be said that the models presented in Eqs. (8) and (9) are more rational than those given in Eq. (7) as former models are not dependent on the 28-day conventional concrete strength.

$$(E_c)_t = J_1 [(f'_c)_t]^{J_2} \tag{7}$$

$$(E_c)_{t,UPV} = J_3 [(f'_c)_{t,UPV}]^{J_4} \tag{8}$$

$$(E_c)_{t,RHN} = J_5 [(f'_c)_{t,RHN}]^{J_6} \tag{9}$$

where $(E_c)_t$ = concrete elastic modulus at age ‘t’ in GPa; $(E_c)_{t,UPV}$ = concrete elastic modulus at age ‘t’ using UPV in GPa; $(E_c)_{t,RHN}$ = concrete elastic modulus at age ‘t’ using RHN in GPa; J_1 to J_6 = model parameters having values 3.739, 0.564, 3.660, 0.571, 3.665, and 0.571, respectively.

The comparison between predicted static elastic modulus obtained from proposed models using Eqs. (7), (8), and

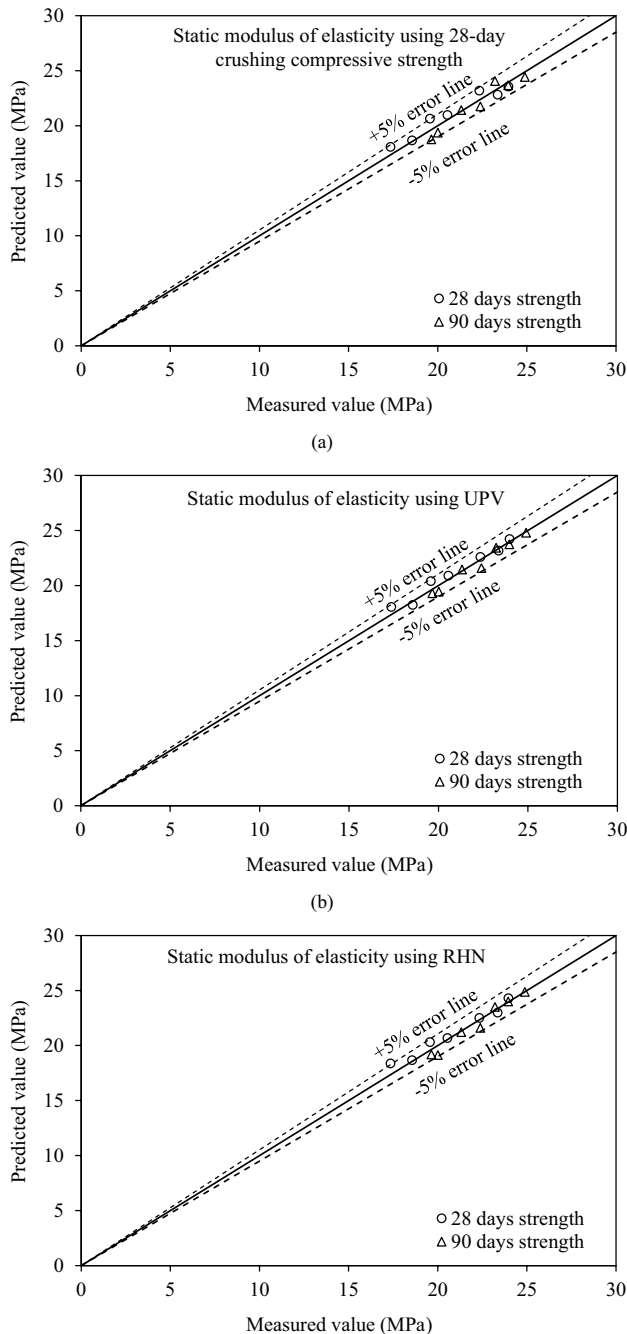


Fig. 11 Comparison between measured and predicted static modulus of elasticity of concrete mixtures evaluated in this study: **a** prediction using 28-day compressive strength; **b** prediction using UPV; and **c** prediction using RHN

(9) and the measured laboratory results for the concrete mixtures evaluated in this study is shown in Fig. 11a–c, respectively. Using these models, an error band of $\pm 5\%$ has also been plotted in the figures. These figures show

that 93%, 100%, and 93% of data lie within the error bands of $\pm 5\%$, using Eqs. (7), (8), and (9), respectively. This indicates that the proposed models for predicting the static elastic modulus of RCA- and BA-based concrete agree with the experimental results and can be applied in the design and construction of concrete buildings prepared with any combination of RCA and BA.

Conclusions

In this study, the conventional concrete has been redesigned by partial and total replacement of natural crushed rock (i.e., coarse aggregate) with RCA and natural riverbed sand (i.e., fine aggregate) with coal BA to examine the mechanical properties of concrete containing different percentages of RCA, BA, and RCA + BA at 28 and 90 days of curing. Keeping in view the experimental research, the following inferences have been drawn:

- The experimentally obtained strengths (compressive and split tensile) and modulus of elasticity of concrete containing RCA and BA are comparable to that of conventional concrete. Thus, the partial or total replacement of natural coarse and fine aggregate with RCA, BA, and their combination can be used to construct sustainable concrete.
- It has been observed that the strengths and modulus of elasticity of 100% RCA at 90 days are similar to the 28 days of conventional concrete properties. The experimental findings are also well supported by SEM analysis. Thus, from laboratory results, the optimum mix is M3 among all concrete mixtures evaluated in this study.
- The proposed age-dependent empirical models based on 28-day compressive strength, UPV, and RHN values used to predict the compressive strength, splitting tensile strength, and modulus of elasticity of RCA, BA, and RCA + BA concrete are found in good agreement with the test results.
- The proposed models can predict the strengths and modulus of elasticity of existing concrete structures prepared with RCA, BA, or RCA + BA at any age without knowing the laboratory test results.
- The present study will be helpful for designers and practicing engineers for fixing preliminary dimensions of reinforced and pre-stressed concrete members made with RCA, BA, or RCA + BA concrete mixes. Moreover, the suggested models will benefit the health assessment of RCA and BA concrete buildings.

- The present study will also be helpful in controlling the use of natural resources such as crushed rock aggregate in concrete construction and resolving the disposal and environmental issues associated with construction and demolition wastes and industrial by-product wastes such as coal bottom ash.
- Further investigations are required on the structural behavior of reinforced concrete containing RCA, BA, or their combination.

Author Contributions AS did visualization, investigation, methodology, and writing—original draft. MS performed conceptualization, software, validation, writing—reviewing and editing. SSS was involved in data curation, investigation, and writing—original draft. MAA done supervision, writing—reviewing and editing.

Funding The authors declare that no funds, grants, or other support were received during the preparation of this manuscript.

Declarations

Conflict of interest On behalf of all authors, the corresponding author states that there is no conflict of interest. The authors have no relevant financial or non-financial interests to disclose.

Ethical approval This article does not contain any studies with human participants or animals performed by any of the authors.

Informed consent For this type of study formal consent is not required.

References

- Zamani AA, Ahmadi M, Dalvand A, Aslani F (2023) Effect of single and hybrid fibers on mechanical properties of high-strength self-compacting concrete incorporating 100% waste aggregate. *J Mater Civ Eng* 35(1):04022365. [https://doi.org/10.1061/\(ASCE\)MT.1943-5533.0004528](https://doi.org/10.1061/(ASCE)MT.1943-5533.0004528)
- Ahmadi M, Abdollahzadeh E, Kioumars M (2023) Using marble waste as a partial aggregate replacement in the development of sustainable self-compacting concrete. *Mater Today: Proc* (available online). <https://doi.org/10.1016/j.matpr.2023.04.103>
- Makul N, Fediuk R, Amran M, Zeyad AM, Murali G, Vatin N, Klyuev S, Ozbakkaloglu T, Vasilev Y (2021) Use of recycled concrete aggregates in production of green cement-based concrete composites: a review. *Crystals* 11(3):232. <https://doi.org/10.3390/cryst11030232>
- Xing W, Tam VW, Le KN, Hao JL, Wang J (2022) Life cycle assessment of recycled aggregate concrete on its environmental impacts: a critical review. *Constr Build Mater* 317:125950. <https://doi.org/10.1016/j.conbuildmat.2021.125950>
- Akhtar A, Sarmah AK (2018) Construction and demolition waste generation and properties of recycled aggregate concrete: a global perspective. *J Clean Prod* 186:262–281. <https://doi.org/10.1016/j.jclepro.2018.03.085>
- McNeil K, Kang THK (2013) Recycled concrete aggregates: a review. *Int J Concr Struct Mater* 7:61–69. <https://doi.org/10.1007/s40069-013-0032-5>
- Tangchirapat W, Buranasing R, Jaturapitakkul C, Chindaprasit P (2008) Influence of rice husk–bark ash on mechanical properties of concrete containing high amount of recycled aggregates. *Constr Build Mater* 22(8):1812–1819. <https://doi.org/10.1016/j.conbuildmat.2007.05.004>
- Sagoe-Crentsil KK, Brown T, Taylor AH (2001) Performance of concrete made with commercially produced coarse recycled concrete aggregate. *Cem Concr Res* 31(5):707–712. [https://doi.org/10.1016/S0008-8846\(00\)00476-2](https://doi.org/10.1016/S0008-8846(00)00476-2)
- Ann KY, Moon HY, Kim YB, Ryou J (2008) Durability of recycled aggregate concrete using pozzolanic materials. *Waste Manag* 28(6):993–999. <https://doi.org/10.1016/j.wasman.2007.03.003>
- Wang HL, Wang JJ, Sun XY, Jin WL (2013) Improving performance of recycled aggregate concrete with superfine pozzolanic powders. *J Cent South Univ* 20(12):3715–3722. <https://doi.org/10.1007/s11771-013-1899-7>
- Ebadi-Jamkhaneh M, Ahmadi M, Kontoni DN (2021) Experimental study of the mechanical properties of burnt clay bricks incorporated with plastic and steel waste materials. In: *IOP Conference series: earth and environmental science* 899(1):012042. <https://doi.org/10.1088/1755-1315/899/1/012042>
- Abdellatif M, Elemam WE, Alanazi H, Tahwia AM (2023) Production and optimization of sustainable cement brick incorporating clay brick wastes using response surface method. *Ceram Int* 49(6):9395–9411. <https://doi.org/10.1016/j.ceramint.2022.11.144>
- Tahwia AM, Abd Ellatif M, Heneigel AM, Abd Elrahman M (2022) Characteristics of eco-friendly ultra-high-performance geopolymer concrete incorporating waste materials. *Ceram Int* 48(14):19662–19674. <https://doi.org/10.1016/j.ceramint.2022.03.103>
- Mohammed AA, Ahmed HU, Mosavi A (2021) Survey of mechanical properties of geopolymer concrete: a comprehensive review and data analysis. *Mater* 14(16):4690. <https://doi.org/10.3390/ma14164690>
- Ahmed HU, Faraj RH, Hilal N, Mohammed AA, Sherwani AF (2021) Use of recycled fibers in concrete composites: a systematic comprehensive review. *Compos B Eng* 215:108769. <https://doi.org/10.1016/j.compositesb.2021.108769>
- Unis H, Mohammed AS, Faraj RH, Qaidi SM, Mohammed AA (2022) Compressive strength of geopolymer concrete modified with nano-silica: experimental and modeling investigations. *Case Stud Constr Mater* 16:e01036. <https://doi.org/10.1016/j.cscm.2022.e01036>
- Singh G (2023) Microstructural and other properties of copper slag–coal bottom ash incorporated concrete using fly ash as cement replacement. *Innov Infrastruct Solut* 8(2):78. <https://doi.org/10.1007/s41062-023-01051-7>
- Li Z, Zhang W, Jin H, Fan X, Liu J, Xing F, Tang L (2023) Research on the durability and sustainability of an artificial lightweight aggregate concrete made from municipal solid waste incinerator bottom ash (MSWIBA). *Constr Build Mater* 365:129993. <https://doi.org/10.1016/j.conbuildmat.2022.129993>
- Sor H, Nadhim NH, Hemn FRH, Ahmed U, Aryan FH, Sherwani, (2021) Experimental and empirical evaluation of strength for sustainable lightweight self-compacting concrete by recycling high volume of industrial waste materials. *Eur J Environ Civ*. <https://doi.org/10.1080/19648189.2021.1997827>
- Oh DY, Noguchi T, Kitagaki R, Park WJ (2014) CO₂ emission reduction by reuse of building material waste in the Japanese

- cement industry. *Renew Sustain Energy Rev* 38:796–810. <https://doi.org/10.1016/j.rser.2014.07.036>
21. Benhelal E, Zahedi G, Shamsaei E, Bahadori A (2013) Global strategies and potentials to curb CO₂ emissions in cement industry. *J Clean Prod* 51:142–161. <https://doi.org/10.1016/j.jclepro.2012.10.049>
 22. Chimenos JM, Segarra M, Fernández M, Espiell F (1999) Characterization of the bottom ash in municipal solid waste incinerator. *J Hazard Mater* 64(3):211–222. [https://doi.org/10.1016/S0304-3894\(98\)00246-5](https://doi.org/10.1016/S0304-3894(98)00246-5)
 23. Singh M, Siddique R (2016) Effect of coal bottom ash as partial replacement of sand on workability and strength properties of concrete. *J Clean Prod* 112:620–630. <https://doi.org/10.1016/j.jclepro.2015.08.001>
 24. Central Electricity Authority (2021) Report on fly ash generation at coal/lignite based thermal power stations and its utilization in the country for the year 2020–21. Thermal Civil Design Division, New Delhi. <https://cea.nic.in>
 25. Ghafoori N, Buchole J (1997) Properties of high-calcium dry bottom ash for structural concrete. *Mater J* 94(2):90–101. <https://doi.org/10.14359/289>
 26. Aggarwal P, Aggarwal Y, Gupta SM (2007) Effect of bottom ash as replacement of fine aggregates in concrete. *Asian J Civ Eng* 8:49–62
 27. Kim HK, Lee HK (2011) Use of power plant bottom ash as fine and coarse aggregates in high-strength concrete. *Constr Build Mater* 25(2):1115–1122. <https://doi.org/10.1016/j.conbuildmat.2010.06.065>
 28. Yang IH, Park J, LeN D, Jung S (2020) Strength properties of high-strength concrete containing coal bottom ash as a replacement of aggregates. *Adv Mater Sci Eng*. <https://doi.org/10.1155/2020/4246396>
 29. Singh N, Mithulraj M, Arya S (2019) Utilization of coal bottom ash in recycled concrete aggregates based self compacting concrete blended with metakaolin. *Resour Conserv Recycl* 144:240–251. <https://doi.org/10.1016/j.resconrec.2019.01.044>
 30. Kumar P, Singh N (2020) Influence of recycled concrete aggregates and Coal Bottom Ash on various properties of high volume fly ash-self compacting concrete. *J Build Eng* 32:101491. <https://doi.org/10.1016/j.jobbe.2020.101491>
 31. Jurič B, Hanžič L, Ilić R, Samec N (2006) Utilization of municipal solid waste bottom ash and recycled aggregate in concrete. *Waste Manag* 26(12):1436–1442. <https://doi.org/10.1016/j.wasman.2005.10.016>
 32. Pal S, Shariq M, Abbas H, Pandit AK, Masood A (2020) Strength characteristics and microstructure of hooked-end steel fiber reinforced concrete containing fly ash, bottom ash and their combination. *Constr Build Mater* 247:118530. <https://doi.org/10.1016/j.conbuildmat.2020.118530>
 33. Hashmi AF, Shariq M, Baqi A (2022) Age-dependent strength assessment of low calcium fly ash concrete based on ultrasonic pulse velocity and rebound hammer number measurement. *IJST-T CIV ENG* 46(6):4327–4341. <https://doi.org/10.1007/s40996-022-00905-x>
 34. Shariq M, Pal S, Chaubey R, Masood A (2022) An experimental and analytical study into the strength of hooked-end steel fiber reinforced HVFA concrete. *Adv Concr Constr* 13(1):35–43. <https://doi.org/10.12989/acc.2022.13.1.035>
 35. Faraj RH, Mohammed AA, Omer KM (2022) Ahmed HU (2022) Soft computing techniques to predict the compressive strength of green self-compacting concrete incorporating recycled plastic aggregates and industrial waste ashes. *Clean Technol Environ Policy* 24(7):2253–2281. <https://doi.org/10.1007/s10098-022-02318-w>
 36. Ahmed HU, Abdalla AA, Mohammed AS, Mohammed AA, Mosavi A (2022) Statistical methods for modeling the compressive strength of geopolymer mortar. *Mater* 15(5):1868. <https://doi.org/10.3390/ma15051868>
 37. IS 4031 (1988) Methods of physical tests for hydraulic cement. Bureau of Indian Standards, New Delhi.
 38. IS 383 (2002) Coarse and fine aggregate for concrete- Specifications. Bureau of Indian Standards, New Delhi.
 39. IS 10262 (2009) Recommended guidelines for concrete mix design. Bureau of Indian Standards, New Delhi.
 40. IS 516 (2004) Indian Standard methods of tests for strength of concrete. Bureau of Indian Standards, New Delhi.
 41. IS 5816 (1970) Method of test for Splitting tensile strength of concrete. Bureau of Indian Standards, New Delhi.
 42. ASTM C469 (2014) Standard test method for static modulus of elasticity and Poisson's ratio of concrete in compression. West Conshohocken, PA, ASTM International.
 43. IS 13311 Part II (1992) Non-destructive testing of concrete-Rebound Hammer. Bureau of Indian Standards, New Delhi.
 44. Singh M, Siddique R (2013) Effect of coal bottom ash as partial replacement of sand on properties of concrete. *Resour Conserv Recycl* 72:20–32. <https://doi.org/10.1016/j.resconrec.2012.12.006>
 45. BS 1881 Part 202 (1986) Recommendations for surface hardness tests by the Rebound Hammer. British Standards Institution, UK.
 46. Teodoru GV (1989) Use of simultaneous nondestructive tests to predict the compressive strength of concrete. Special Publication 112:137–152. <https://doi.org/10.14359/3715>
 47. Neville AM (1995) Properties of concrete. Longman, London
 48. IS 13311 Part I (1992) Non-destructive testing of concrete-Ultrasonic Pulse Velocity. Bureau of Indian Standards, New Delhi
 49. Khatib JM (2005) Properties of concrete incorporating fine recycled aggregate. *Cem Concr Res* 35(4):763–769. <https://doi.org/10.1016/j.cemconres.2004.06.017>
 50. Gholampour A, Ozbakkaloglu T (2018) Time-dependent and long-term mechanical properties of concretes incorporating different grades of coarse recycled concrete aggregates. *Eng Struct* 157:224–234. <https://doi.org/10.1016/j.engstruct.2017.12.015>
 51. Cheriaf M, Rocha JC, Pera J (1999) Pozzolanic properties of pulverized coal combustion bottom ash. *Cem Concr Res* 29(9):1387–1391. [https://doi.org/10.1016/S0008-8846\(99\)00098-8](https://doi.org/10.1016/S0008-8846(99)00098-8)
 52. Singh N, Bhardwaj A (2020) Reviewing the role of coal bottom ash as an alternative of cement. *Constr Build Mater* 233:117276. <https://doi.org/10.1016/j.conbuildmat.2019.117276>
 53. Muthusamy K, Rasid MH, Jokhio GA, Budiea AMA, Hussin MW, Mirza J (2020) Coal bottom ash as sand replacement in concrete: a review. *Constr Build Mater* 236:117507. <https://doi.org/10.1016/j.conbuildmat.2019.117507>
 54. Andrade LB, Rocha JC, Cheriaf M (2007) Aspects of moisture kinetics of coal bottom ash in concrete. *Cem Concr Res* 37(2):231–241. <https://doi.org/10.1016/j.cemconres.2006.11.001>
 55. Nakararaj N, Tran TNH, Sukontasukkul P, Attachaiyawuth A, Tangchirapat W, Ban CC, Jaturapitakkul C (2022) Effects of high-volume bottom ash on strength, shrinkage, and creep of high-strength recycled concrete aggregate. *Constr Build Mater* 356:129233. <https://doi.org/10.1016/j.conbuildmat.2022.129233>
 56. Mistri A, Bhattacharyya SK, Dhama N, Mukherjee A, Barai SV (2019) Petrographic investigation on recycled coarse aggregate and identification the reason behind the inferior performance.

- Constr Build Mater 221:399–408. <https://doi.org/10.1016/j.conbuildmat.2019.06.085>
57. Yap SP, Alengaram UJ, Jumaat MZ, Khaw KR (2016) Torsional and cracking characteristics of steel fiber-reinforced oil palm shell lightweight concrete. *J Compos Mater* 50(1):115–128. <https://doi.org/10.1177/0021998315571431>
 58. Yuksel I, Genç A (2007) Properties of concrete containing non-ground ash and slag as fine aggregate. *ACI Mater J* 104(4):397. <https://doi.org/10.14359/18829>
 59. Abdellatif M, Alanazi H, Radwan MK, Tahwia AM (2022) Multiscale characterization at early ages of ultra-high performance geopolymer concrete. *Polym* 14(24):5504. <https://doi.org/10.3390/polym14245504>
 60. Abdellatif M, AL-Tam SM SM, Elemam WE, Alanazi H, Elgendy GM, Tahwia AM (2023) Development of ultra-high-performance concrete with low environmental impact integrated with metakaolin and industrial wastes. *Case Stud. Constr. Mater* 18:e01724. <https://doi.org/10.1016/j.cscm.2022.e01724>
 61. Tahwia AM, Abd Ellatif M, Bassioni G, Heniegal AM, Abd Elrahman M (2023) Influence of high temperature exposure on compressive strength and microstructure of ultra-high performance geopolymer concrete with waste glass and ceramic. *J Mater Res Technol* 23:5681–5697. <https://doi.org/10.1016/j.jmrt.2023.02.177>
 62. Singh M, Siddique R (2014) Strength properties and micro-structural properties of concrete containing coal bottom ash as partial replacement of fine aggregate. *Constr Build Mater* 50:246–256. <https://doi.org/10.1016/j.conbuildmat.2013.09.026>
 63. Rafeizonooz M, Mirza J, Salim MR, Hussin MW, Khankhaje E (2016) Investigation of coal bottom ash and fly ash in concrete as replacement for sand and cement. *Constr Build Mater* 116:15–24. <https://doi.org/10.1016/j.conbuildmat.2016.04.080>

Springer Nature or its licensor (e.g. a society or other partner) holds exclusive rights to this article under a publishing agreement with the author(s) or other rightsholder(s); author self-archiving of the accepted manuscript version of this article is solely governed by the terms of such publishing agreement and applicable law.